EDGE2D-EIRENE modelling of the impact of wall materials on core edge, scrape-off layer and divertor parameters

A.V. Chankin[a], G. Corrigan[b] and JET Contributors*

EUROfusion Consortium, JET, Culham Science Centre, Abingdon, OX14 3DB, UK
[a]Max-Planck-Institut für Plasmaphysik, Garching bei München, Germany
[b]CCFE, Culham Science Centre, Abingdon, UK

Abstract

A series of EDGE2D-EIRENE cases, based initially on the case simulating JET L-mode plasma with ITER-like wall (ILW) with the input power close to the H-mode power threshold, was run in different wall environments. They included ILW, with tungsten (W) covering the divertor, and beryllium (Be) – main chamber surfaces, all carbon (C) and all W walls. Contrary to expectations based on the idea that deeper penetration of neutrals re-emitted from surfaces with higher atomic mass into the plasma core raises core density, EDGE2D-EIRENE cases had the highest density in the C wall case. This is explained via the effect of the 'power deficit' in the divertor, as recycling neutrals deposit a fraction of their power into walls, thereby cooling the divertor plasma. This effect is stronger in C compared to W divertor surfaces. The plasma cooling in the divertor increases plasma density and neutral recycling, with more neutrals penetrating into the core. Metal wall (ILW and W wall) EDGE2D-EIRENE cases were found to have larger radial electric field (E_r) both inside and outside of the separatrix, in line with the mechanism of the E×B shear turbulence suppression and experimental observations of lower H-mode power threshold in metal wall machines. The originally expected trend for higher core densities in metal wall machines, based on the effect of deeper penetration of neutrals re-emitted from higher atomic mass surfaces, was recovered in much lower density EDGE2D-EIRENE cases, where the effect of the power deficit in the divertor was less important. Subtle effects of interplay among mechanisms involving neutral circulation in the divertor and in the main chamber wall are considered to explain differences between ILW and W wall cases.

*See the author list of "Overview of the JET preparation for Deuterium-Tritium Operation", by Joffrin E. *et al* 2019 Nucl. Fusion **59**, 112021

1. Introduction

The most commonly used scaling to predict the H-mode power threshold in tokamaks, P_{LH}, in particular in future fusion experiments such as ITER and DEMO, is Martin's scaling [1]. It contains dependencies on the machine size (area of the last closed flux surface), toroidal magnetic field and line averaged electron plasma density, applicable in the high density branch (where P_{LH} increases with density, contrary to the low density branch where P_{LH} increases with the decrease of density), considered to be of relevance for the operation of the fusion reactor. In addition, it is also known that P_{LH} depends on the hydrogen isotope, being approximately inversely proportional to the isotope mass (see e.g. [2,3]).

More recently it was observed that JET operation in the ITER-like wall (ILW), with tungsten (W) covering divertor surfaces, including target plates, and beryllium (Be) covering the main chamber wall, led to a reduction of P_{LH} by ~ 30% (and by ~40% when the radiation from the bulk plasma was subtracted), compared to the earlier operation in the carbon (C) wall environment, where C covered all material surfaces facing plasma and neutral particles [4]. Lower P_{LH}, by 25%, was also found in ASDEX Upgrade (AUG) with the full W wall, compared to earlier discharges in the mixed graphite (C) and W environment [5].

In JET experiments, for the same edge plasma density the L–H transition occurred at lower edge electron temperature, T_e, and electron pressure, p_e, in ILW than in C wall [4]. At the same time, in AUG lower P_{LH} in full W discharges was obtained at higher edge density, steeper edge density profile, higher gas puff and higher degree of detachment [5]. The calculated minimum in the neoclassical radial electric field, E_r, inside the separatrix was found to be the same in both wall environments before the L-H transition [5], supporting the mechanism of turbulence suppression by sheared poloidal E×B rotation [6,7] and leading to a better particle and energy confinement.

A tentative explanation of lower P_{LH} in JET ILW plasmas compared to C wall plasmas was proposed in [8,9] based on runs with EDGE2D-EIRENE, which is a code package combining coupled plasma 2D edge fluid code EDGE2D and neutral Monte-Carlo code EIRENE [10-12]. As a starting point these runs simulated an L-mode JET plasma prior to the L-H transition with the plasma edge density profile, input power (P_{in}) and divertor configuration ('VH') corresponding to experimental conditions. The EDGE2D-EIRENE modelling was then extended assuming all C environment while maintaining the same separatrix electron density, $n_{e,sep}$, which required lower gas puff rates in the C wall case. The same P_{in} into the computational grid and the same anomalous transport coefficients were used in both cases, resulting in the same E_r inside

the separatrix. The ILW case however had a larger E_r spike in the near scrape-off layer (SOL) at the outer midplane (OMP), which was related with higher particle and energy reflection coefficients for ions and neutrals impinging on the W target compared to the C target. Compared to the W wall, the C wall divertor provides a stronger energy sink leading to an extra cooling of both neutrals and plasma in the divertor resulting in lower T_e at divertor targets, which in turn gives rise to lower upstream (at OMP) E_r. Contrary to the standard explanation of the turbulence suppression, based on the sheared E×B flows inside of the separatrix, the explanation in [8,9] invoked a possibility of the turbulence suppression triggered by larger E×B shear outside of the separatrix in the near SOL.

In order to understand AUG results, a series of EMC3-EIRENE runs was carried out by exploiting the same idea of different reflection coefficients from C and W surfaces [13]. EMC3-EIRENE is a code package coupling the plasma fluid 3D code with EIRENE, the details of the EMC3 code and the coupling between the two codes are described in [14,15]. The emphasis in this modelling was on density profiles, and its results supported the original idea [5] that higher reflection coefficients from W surfaces result in longer mean free paths of more energetic neutrals leading to higher ionization rate inside of the separatrix, thus raising density and its gradient there, in line with experimental observations in AUG. The EMC3-EIRENE results were particularly clear in cases with low density achieved without the gas puff, whereas in high density cases the difference between W and C cases was strongly reduced. This was explained by a much lower divertor T_e, with energies of neutrals re-emitted from material surfaces being low, so that the dominant process to produce neutrals in the ~eV range was molecular dissociation. The contribution of neutrals originating due to molecular dissociation to the total neutral flux across the separatrix was of the same order as that from neutrals re-emitted from divertor targets.

In AUG experiments higher plasma density is obtained in the W wall environment compared to the C environment. This is seen both in plasmas without the gas puff and with the gas puff [16]. Apart from explanations of this observation given above, a number of other mechanisms was analyzed in [16] (note that Ref. [16] was published before [13]). In particular, the authors of [16] point out that carbon has a better pumping capability, being able to store more deuterium during the discharge, with its consequent release in between discharges, leading to a reduced density during the discharge. Lower hydrogen isotope retention in metallic walls is a well known effect [17,18]. At the same time, since SOL density was the same in W and C walls, it is possible that higher (core and pedestal) density in the W case was caused by improved particle confinement in the core [16].

Contrary to AUG results, in the JET high power H-mode pulse in ILW, made to re-create conditions of an earlier pulse in the C environment, both line-averaged and edge electron densities, averaged over the entire duration of the pulse, including the effect of ELMs, were found to be lower than in the C pulse [19]. The two pulses were separated by only ~ 2 year time gap from each other, and the settings of the ILW pulse were exactly the same as in the C wall pulse, including the same gas puff rate [20]. Analysis of inter-ELM data revealed that the density at the top of the pedestal was also higher in the C wall pulse [20].

It has to be pointed out that neither EDGE2D nor EMC3 codes model turbulence, with both using user specified anomalous transport coefficients for perpendicular/radial plasma particle and power fluxes. Therefore the only meaningful modelling using these codes can be aimed at comparisons of density (e.g. the electron density n_e) and ion and electron temperature ($T_{e,i}$) profiles for the same plasma transport coefficients, but with different wall materials (C,W,Be). EDGE2D solutions can also yield electric potential and electric field profiles when cases are run with classical drifts switched on. In this paper EDGE2D-EIRENE cases modelling JET conditions are run for three different wall conditions: ILW, all C wall and all W wall. In both EDGE2D-EIRENE and EMC3-EIRENE runs the TRIM database for coefficients describing interaction of the plasma and neutrals with material surfaces is used, which is incorporated into EIRENE. Further details with examples of reflection coefficients are given in [13].

In this paper the setup of EDGE2D-EIRENE cases is described in Sec. 2. Modelling results of global plasma parameters and OMP profiles are presented in Sec. 3. Target profiles, neutral recycling and power balance in the SOL and divertor are discussed in Sec. 4. Output E_r profiles at OMP are presented in Sec. 5. Since EDGE2D-EIRENE cases with drifts are prone to numerical instabilities, especially at high $T_{e,i}$ in the divertor, running lower density cases enforced switching drifts off. To test the influence of drifts on code solutions, the ILW, C and W wall cases are repeated without drifts, with results of these cases presented in Sec. 6. After that, lower density cases but with the same input power were run without drifts, with results presented in Sec. 7. The summary of the work is given in Sec. 8.

2. Setup of EDGE2D-EIRENE cases

For each choice of input parameters two EDGE2D-EIRENE cases were first run in ILW and C wall environments. Despite JET never operated in the all W environment, for completeness EDGE2D-EIRENE cases were then also run assuming full W wall.

In all cases pure deuterium (D) plasma was specified. The influence of different wall materials

on the cases was only in creating different particle and energy reflection coefficients of ions and neutrals interacting with exposed material surfaces. The preference for pure D cases was motivated by the desire to simplify EDGE2D-EIRENE setups enabling one to focus on the influence of neutral and ion reflection coefficients from different surfaces. Otherwise code results could have been masked by other effects. For example, in C wall cases carbon can radiate a significant amount of power, mainly in the divertor. At the same time, in ILW cases Be from the main chamber wall is typically a weak radiator, with line radiation below that from D. And tungsten radiation can almost always be neglected. When this is not the case, the concentration of highly charged W impurities in the plasma core is too high, causing an unacceptable power loss due to W radiation, so that almost no power to the SOL plasma is left. Therefore, comparing e.g. ILW and C wall EDGE2D-EIRENE cases where radiating impurities are included in the ion plasma mix would create different plasma conditions in the SOL and divertor making it difficult to separate out effects of surface reflection coefficients.

The basis for all cases described in this paper served an earlier case described in [8,9], corresponding to JET L-mode conditions of the pulse #81883 with toroidal magnetic field B_t = 2.4T and plasma current I_p = 2MA, in the 'HT' divertor configuration, with the inner strike point on the vertical, and outer – on the horizontal target (see Fig. 1 below). This case was simulated with EDGE2D-EIRENE using experimental profiles prior to the L-H transition in the high density branch. The magnetic configuration in the divertor and the EDGE2D grid used for the plasma modelling can be found in Figs. 1 and 2 of [9], respectively. Here, an expansion of the grid around the divertor region is shown in Fig. 1. Unlike in [9], where $n_{e,sep}$ was maintained at a fixed value by a combination of the gas puff from the private flux region and wall recycling, which required different puff rates for different cases, in this study the setup of all cases was exactly the same. All cases had the same deuterium gas puff rate, 4.2×10^{21} s^{-1} (in electrons per second), introduced from the top of the machine, 3 MW of neutral beam injection (NBI) input power (P_{in}) into the EDGE2D grid, introduced from the inner core boundary and split equally between ion and electron channels. In addition, 0.85×10^{20} s^{-1} of the 'core fuelling' was introduced from the inner core boundary, accounting for the ionization source from NBI. Spatially constant

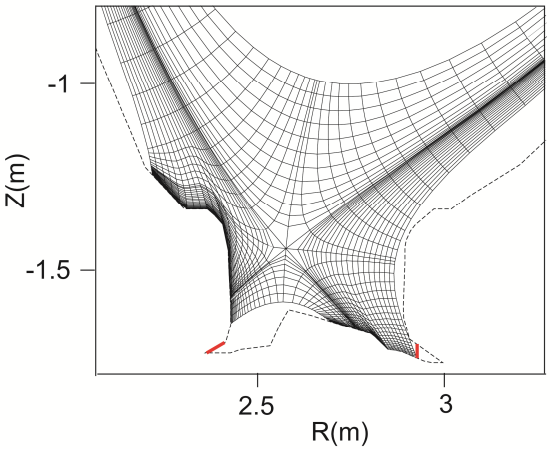

Fig. 1. Expansion of the EDGE2D grid around the divertor, with positions of pump surfaces indicated in red.

anomalous transport coefficients were used: diffusion coefficient $D_\perp$=1 m^2s^{-1} and electron and ion heat conductivities $\chi_{e,i}$=2 m^2s^{-1}. Particle and power fluxes to material surfaces outside the EDGE2D grid were calculated assuming a radial density decay length of 1 cm. Dedicated tests showed code results to be rather insensitive to the decay length [21]. Plasma particle balance inside of the EDGE2D grid was maintained by gas puffing and pumping of neutrals by artificial pump surfaces with the fixed albedo, placed in the corners of inner and outer divertors as shown by red segments in Fig. 1, approximately emulating pumping by the cryo-pump. Other, more specific details of the setup of EDGE2D-EIRENE cases can be found in [9]. The choice of the same gas puff rate seems more natural compared to maintaining constant $n_{e,sep}$, as the results can better reveal the causality among various processes, where different values of $n_{e,sep}$ obtained in different cases come as a result that has to be explained by physics contained in EDGE2D-EIRENE. The choice of a pure D plasma, without impurities sputtered from exposed material surfaces, allows one to focus on the effect of reflection rates from different surfaces.

In the first series of cases described in this paper classical drifts were switched on. A self-consistent neoclassical model for E_r was implemented in the core which impeded surface averaged radial currents. In the SOL and divertor, the primary quantity calculated in the EDGE2D is electric potential in the plasma, with the divertor target potential assumed to be zero.

3. Outer midplane (OMP) profiles and global parameters

All three EDGE2D-EIRENE cases reached steady state conditions, where parameters stopped evolving. Radial profiles of n_e, T_e and T_i at the OMP position are plotted in Fig. 2. The C wall case has a substantially higher density across the whole grid compared to the other two cases, to be often referred to as 'metal wall cases' below. Correspondingly (given fixed P_{in} and transport coefficients) this case has lower temperatures. The W wall case has similar profiles to the ILW case, but the density is slightly higher (while temperatures - lower) than in the ILW case.

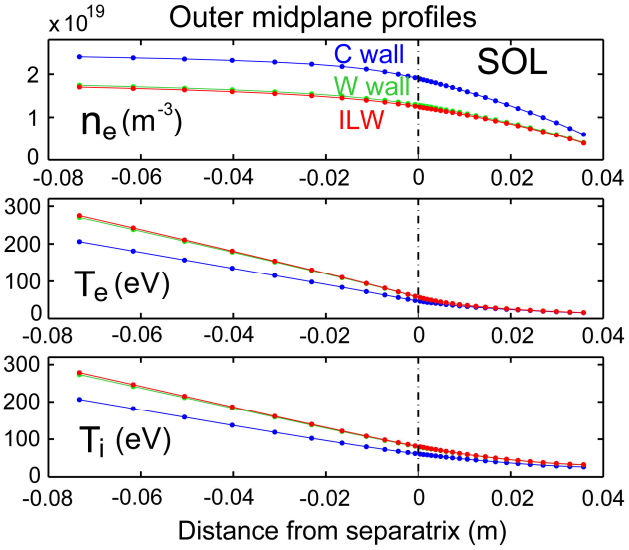

Fig. 2. Radial profiles of plasma parameters at the OMP position.

A substantially higher $n_{e,sep}$ in the C wall case implies higher neutral ionization in the core. Since

in the steady state conditions the neutral flux into the core is balanced by the plasma flux from the core into the SOL across the separatrix, a substantially higher plasma flux into the SOL is crossing the separatrix in the C wall case. This flux is mostly described by the diffusive plasma particle flux given by the $-D_{\perp}\nabla n$ term (remember that ion and electron densities are equal in these runs), with the particle flux caused by drifts being much smaller. Due to different density gradients this flux ('ion particle flux' in the EDGE2D output) is: 1.00×10^{22}, 1.45×10^{22} and 1.074×10^{22} s^{-1} for ILW, C and W wall cases, respectively.

Ion and electron pressure profiles in the core region for the three cases are almost identical, since the variation of density gradients is compensated by the variation of temperatures gradients, as expected for fixed P_{in} and transport coefficients. The cause of the differences in OMP profiles is discussed in the next section.

4. Target parameters, neutral recycling and power balance in the SOL and divertor

Electron density and electron and ion temperatures at divertor targets for the three cases analyzed are plotted in Fig. 3. The most significant difference is between the C wall case and metal wall cases. In particular, in the C wall case target T_e and T_i are very low, while n_e is mostly higher than in ILW and W wall cases. We shall first discuss this main difference, and only later – the smaller difference between ILW and W wall cases.

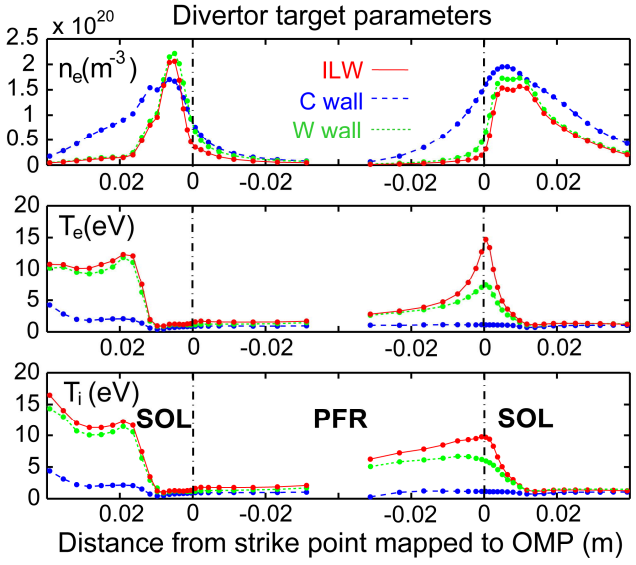

Fig.3. Divertor target profiles vs. distance from strike points mapped to the OMP position.

The trigger for the strong divergence of the C wall case from the (original) ILW case can only be lower particle and energy reflection coefficients for ions and neutrals impinging on carbon (graphite) surfaces. In order to estimate the impact of this effect on the power balance in the divertor, two additional EDGE2D-EIRENE cases in C and W walls were run. Each of these two cases had only one time step, with the plasma state before this step taken from the ILW case solution. Changes to the plasma state due to only one time step are negligible. The EIRENE output for these cases contains incident and re-emitted neutral power fluxes (predominantly from D atoms, since molecular, D_2, energies were by ~ two orders

of magnitude lower), from all plasma facing surfaces.

For the same incident ion and neutral fluxes, predominantly to divertor targets, the difference between re-emitted power flux in ILW and C wall cases is 158 kW. This power flux represents a deficit of power, or an extra power left in material surfaces by impinging ions and neutrals, in the C case compared to the ILW case. To assess the importance of this 'power deficit', it has to be compared with the power left in the plasma after the subtraction of volume power losses, out of which the main processes are neutral ionization, molecular dissociation, charge exchange and 'hydrogen' (as stated in the EDGE2D-EIRENE output, but actually deuterium) radiation. All these power losses together amount to 1.77 MW in the ILW case. The power remaining in the divertor is obtained by subtracting 1.77 MW from P_{in} = 3 MW, giving 1.23 MW. The power deficit in the C wall case plasma originating from lower energy reflection coefficients, 158 KW, represents 12.8% of P_{in}. By itself it is probably unlikely to cause such a large cooling of the C wall case plasma resulting in a near collapse of target temperatures. There must be other mechanisms, triggered by a change in boundary conditions resulting in the initial power deficit, which, via positive feedback loops, cause much deeper $T_{e,i}$ drops near targets. The most obvious mechanisms are related to an increase in plasma density in the divertor in response to an (initial) cooling of the divertor plasma. Higher density leads to higher neutral recycling in the divertor, increasing volume power losses, leading to lower temperature and higher density, and so on. In the cases analyzed here, recycling in the divertor is higher in the C wall case: total ionization of neutrals, which mostly takes place in the divertor, is: 2.861×10^{23}, 3.680×10^{23} and 3.058×10^{23} s^{-1} for the ILW, C and W wall cases, respectively. In the C wall case, target $T_{e,i}$ near strike points are close to 1eV, plasma pressure doesn't fall significantly from the OMP to targets, and recombination losses are relatively low, 44.9 kW (and only 1.92 kW in the ILW case), compared to total volumetric power losses of 1.898 MW. Hence, there is no evidence of an ongoing detachment.

Higher recycling in the divertor in the C wall raises neutral flux to the main chamber wall, which is equal to 3.65×10^{22}, 5.70×10^{22} and 3.74×10^{22} s^{-1} for ILW, C and W wall cases, respectively. The flux to the main chamber wall is by factor ≈ 1.5 higher in the C wall case than in the metal wall cases.

Fig. 4 shows total neutral ionization sources inside poloidal rings in ILW, C and W wall cases against distance from the separatrix at the OMP position. The 'poloidal ring' is volume composed of adjacent EDGE2D cells (see Fig. 1) in the poloidal direction, in between flux surfaces. Note that the number of cells in poloidal rings is different in the core and in the SOL: in

the latter case also cells in the divertor, between targets and entrances to the divertor, are counted. The volume of each ring includes the toroidal circumference factor $2\pi R$ of each cell, with R being major radius. The total ionization source in the plasma can be calculated by summing up all ionization source values along profiles shown in Fig. 4. Since ionization source profiles in the core region cannot be easily resolved, they are additionally plotted inside of the insert in Fig. 4 showing a zoomed-in part of the profiles in the core. The ionization source is highest in the C wall case, especially in the outer SOL at distances > 0.008 m. A distinct spike in the ionization source in the C wall case at the first two rings in the SOL is caused by neutrals propagating from the divertor towards the core being ionized inside large volume cells close to the X-point. Large spikes in these cells can be seen on ionization source profiles along poloidal distance for rings just inside and outside of the separatrix. These profiles are not shown here.

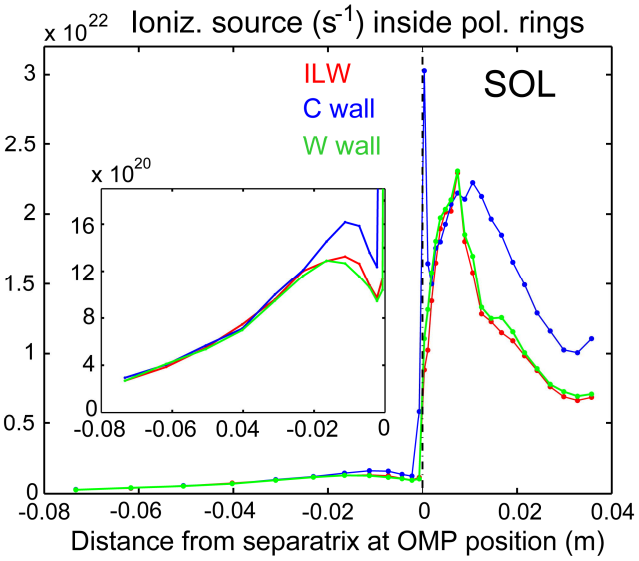

Fig. 4. Neutral ionization source inside poloidal rings vs. distance from separatrix at the OMP position for ILW, C and W wall cases. The insert shows a zoomed-in part of profiles in the core region.

Note that ionization source profiles presented here mainly indicate trends for comparing the three cases, with different wall materials, against each other. By themselves shapes of these profiles may be misleading, for example they show drops in the ionization source towards the separatrix position from both SOL and core sides. This is caused by the effect of different cell sizes owing to compression of the EDGE2D grid towards the separatrix, see Fig. 1.

We shall now discuss the difference in EDGE2D-EIRENE solutions between ILW and W wall cases. The solutions didn't support original expectations based on the comparison between ILW and C wall cases, that further increasing the atomic mass of the surface material, by replacing the Be main chamber wall with the W wall (thereby transitioning from the ILW to the W wall case) would result in a decrease in the core and separatrix densities, leading to higher $T_{e,}$, in the divertor. The EDGE2D-EIRENE result can be understood by taking into consideration that neutrals re-emitted from the main chamber wall, being closer to the separatrix, have higher probability to penetrate through the separatrix and be ionized in the core than those recycling in

the divertor. This should raise core and separatrix densities, leading to lower $T_{e,i}$ shifting W wall case results slightly in the direction of the C wall case. At the same time, since the divertor material (W) is the same for both metal wall cases, the divertor physics aspects discussed above and related to high recycling in the divertor, leading to higher separatrix density in the C wall case, are irrelevant here. A slightly higher separatrix density in the W wall case agrees with slightly higher neutral ionization source in the W wall case at and just outside of the separatrix position, as can be seen in Fig. 4.

Energy reflection coefficients for neutrals circulating at the main chamber wall are approximately 20, 35 and 70% for ILW, C and W wall cases, respectively, as follows from the EIRENE output. Deeper neutral penetration in the W wall compared to the ILW case can not however be clearly seen in Fig. 4. This should probably be attributed to a relatively low contribution of neutrals circulating near the main chamber wall to the total ionization source in the core, since the neutral flux to the main chamber wall is by an order of magnitude lower than the neutral recycling in the divertor, as follows from the fluxes quoted above.

Summarizing, we conclude that the difference between EDGE2D-EIRENE solutions for ILW and W wall cases can be attributed to the mechanism described in refs. [5] and [13] for AUG experiments and EMC3-EIRENE modelling. Deeper penetration of neutrals re-emitted from the wall (in this case, from the main chamber wall) when it is made of heavier material (W, compared to Be) creates larger ionization in the confined region, compared to SOL and divertor regions where particle confinement is much poorer due to charged particles' sink to the target. This results in a (slightly) higher density across the whole computational domain in the W wall case. The close proximity of the ILW to W wall case results may also be caused by the influence of drift effects on recycling in the divertor, which must have been particularly strong in the ILW case, see discussion in Sec. 6.

5. Profiles of radial electric field (E_r) at the OMP position

E_r profiles for the three EDGE2D-EIRENE cases are shown in Fig. 5. Positive E_r spikes in the near SOL can to a large extent be attributed to radially falling T_e and associated electric potential Debye sheath drops ~ $3T_e/e$ which for negative ∇T_e and constant target potential result in positive E_r ~ $-3\nabla T_e/e$ at the OMP position, as in ILW and W wall cases. In the C wall case, owing to very low target T_e other contributions to the E_r at the OMP position may become important, in particular due to radial gradient of the $-\int_{OT}^{OMP} \nabla_{||}(p_e)/en_e ds_{||}$ term, with the

expression in the integral coming from the parallel (along field lines) momentum balance equation, with $s_{||}$ being parallel distance [22]. The first, negative E_r spike in the SOL in the C wall cases is very narrow, covering only the first cell outside of the separatrix. It may be considered an artifact of electric potential and E_r calculations in EDGE2D. As was pointed out in Sec. 2, the primary quantity calculated in the core is E_r, while in the SOL it is electric potential. Owing to a topological discontinuity between core and SOL regions in EDGE2D the link between them is established by equating electric potential in the outermost core cell at the OMP position to that of the innermost cell in the SOL. E_r in the SOL is calculated by subtracting electric potentials in neighboring cells. The contribution due to the term with $\nabla_{||}(p_e)/en_e$ must also be important for positive E_r spikes in the near SOL in C and W wall cases, in particular in the C wall case, otherwise the positive E_r spike in this case would have been factor ~10 smaller than that in the ILW case, based on the comparison of target T_e gradients and assuming the Debye sheath drop being the only mechanism to create the electric potential in the plasma. In reality, in the code output the positive E_r spike in the C wall case is only by factor ≈ 4 smaller than in the ILW case.

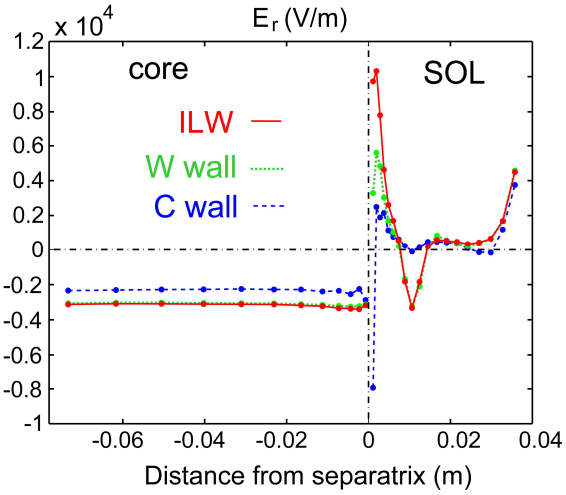

Fig. 5. Radial electric field across outer core and SOL regions at the OMP position.

In the core, E_r is negative, having lower absolute values in the C wall case, despite larger density gradients in this case compared to metal wall cases. This can be explained by the E_r dependence on ion density and temperatures gradients on closed flux surfaces. According to the neoclassical theory, provided there is no toroidal momentum (toroidal momentum is very small in the cases analyzed here, as zero toroidal velocity is specified at the inner core boundary in the EDGE2D-EIRENE cases) the equation for E_r in the plasma core is given by (see e.g. [23]):

$$eE_r = (T_i \nabla n + kn\nabla T_i)/n, \qquad (1)$$

where k is a numerical coefficient which depends on the ion collisionality, and n is plasma density. The coefficient k is equal to 3.1, 1.5 and -0.17 in Pfirsch-Schlüter, Plateau and Banana collisionality regimes, respectively [23]. With classical drifts included in the EDGE2D model, EDGE2D-EIRENE runs have all the physics necessary to correctly calculate neoclassical E_r.

Radially decaying density and T_i profiles imply that E_r must be negative in the core, which is the case in the EDGE2D-EIRENE solutions, as seen in Fig. 5.

Eq. (1) can be recast into:

$$eE_r = [\nabla p_i + (k-1)n\nabla T_i]/n. \qquad (2)$$

Ion pressure profiles are almost the same in all cases, owing to the same P_{in} and transport coefficients specified in EDGE2D. Using $\nabla p_i = n\nabla T_i + T_i\nabla n \approx const$ one can approximately replace the $n\nabla T_i$ term with $-T_i\nabla n$ in the numerator on the right hand side (RHS) of Eq. (2). This makes it clear that higher density gradients lead to more positive E_r, or, in absolute values, higher $|\nabla n|$ lead to lower $|E_r|$, provided the plasma density itself is fixed. This must be valid in Pfirsch-Schlüter and Plateau regimes covering plasma parameters within the EDGE2D grid, since $(k-1)$ is positive in these regimes. This is one of the reasons (but not the most important, see below) for higher $|E_r|$ in the core in the metal wall cases than in the C wall case. The other reason is a substantially higher density in the C wall case, since the density figures in the denominator of Eqs. (1) and (2). EDGE2D equations assume the plasma to be in the Pfirsch-Schlüter collisionality regime inside of the entire computational grid. Calculations of the code E_r values at the OMP position using Eq. (2), with the linear approximation for gradients based on two neighboring cells, shows a high degree of proportionality, within 1%, between calculated and code E_r values for positions in the core region for all cases (ILW,C,W).

It is of interest to assess relative contributions of $T_i\nabla n$ and $n\nabla T_i$ terms to E_r in Eq. (1). Ratios $(n\nabla T_i)/(T_i\nabla n)$ for the second cell inside of the separatrix are 2.31, 2.18 and 2.31 for ILW, C and W wall cases, respectively. Due to the presence of the coefficient $k > 1$ before the $n\nabla T_i$ term its contribution to E_r is dominant, so that one can very approximately assume that E_r in these cases is determined only by ∇T_i. Since the ion temperature gradient is lowest in the C wall case, it has the lowest $|E_r|$. For more inward positions in the core the ratio $(n\nabla T_i)/(T_i\nabla n)$ is higher than quoted above. In particular, for the 5th point, counting from the outer core boundary, which is in the middle of the core region, this ratio is by factor ~ 2 higher.

Precise measurements of edge ion temperature profiles in experiments are scarce. In Ref. [24] from AUG it is reported that $T_i\nabla n$ and $n\nabla T_i$ terms are of the same order of magnitude, and as an estimate the relation $eE_r = 2\nabla T_i$ is used for plasma conditions close to the L-H transition. Generally, in AUG experiments, for small toroidal rotation velocities, E_r is found to be well described by a simple approximation of $\nabla p_i/en$ [25].

It can be argued to which extent modelling results obtained in this work depend on the dominance of the $n\nabla T_i$ term over $T_i\nabla n$, and hence, to which extent these results can be generalized in application to other plasma conditions. Let's consider an opposite, hypothetical situation with the completely flat ion temperature profile, for which from Eq. (1) one obtains: $eE_r = T_i\nabla n/n$, or $|eE_r| = T_i/\lambda_n$, with λ_n being the density decay length. For fixed P_{in} and transport coefficients, at higher densities caused by higher ionization source T_i must be lower. However, much depends on details of the density profile. For example, in cases, or at positions, where the density rise is stronger than the rise of its gradient, or where both n and ∇n rise by the same factor, qualitative conclusions obtained in this work should hold. An opposite case is when ∇n has risen stronger than the density itself, and by a factor larger than the factor of the T_i reduction. Under such conditions higher density may result in higher $|eE_r|$, which would make results qualitatively similar in high and low divertor recycling conditions, and in line with the trend discussed in [5,13]. Such a result however requires certain assumptions about the density profile, in addition to arguments based on higher reflection coefficients from wall materials with higher atomic mass.

One issue with E_r profiles shown in Fig. 5 is that they are flat in the core region. This is in contrast with experimental observations of the E_r 'well' just inside of the separatrix (see e.g. ASDEX Upgrade results in [25]). One reason for this disagreement is related to EDGE2D plasma equations assuming strong collisionality Pfirsch-Schlüter regime for both SOL and core regions, as pointed out above. In reality this assumption is typically violated, as the plasma, being almost always in the Pfirsch-Schlüter regime in the SOL, becomes less collisional more inward, and, within the EDGE2D grid transitions into the Plateau regime. The coefficient $(k-1)$, which accounts for the ∇T_i contribution to E_r in Eq. (2), should therefore be reduced from ≈ 2 to ≈ 0.5 during the transition from the Pfirsch-Schlüter to Plateau regime, making $|E_r|$ smaller for more inward positions, thereby making the E_r profile shape closer to those observed in experiment. The other reason for the E_r 'well' observed in experiments is steepening of the ion pressure profile towards the separatrix (see e.g. E_r and ∇p_i profiles in [25]).

6. The no-drift case and the impact of drifts on EDGE2D-EIRENE solutions

Higher density and its gradient in the C wall EDGE2D-EIRENE case compared to metal wall cases is attributed here to the 'power deficit' in the divertor caused by lower energy reflection coefficients from lower atomic mass wall surfaces. An opposite tendency, for the density and its gradient being higher in the W wall case compared to the C wall case was found in low density

EMC3-EIRENE cases analyzed in [13], as discussed above.

In order to try to reconcile these conflicting results it is necessary to run EDGE2D-EIRENE cases in much lower plasma density conditions, with a much lower neutral recycling in the divertor, where the power deficit effect is strongly diminished.

In lower density cases the effect of deeper penetration into the core of neutrals reflected from higher atomic mass surfaces, raising core density, as discussed in [5,13], may be expected to show itself also in EDGE2D-EIRENE solutions. Results of lower density EDGE2D-EIRENE cases will be presented in Sec. 7. Since owing to numerical instabilities related to high target T_e such cases could not be run with drifts, it is important to verify whether conclusions based on running the EDGE2D-EIRENE drift cases critically depend on the presence of drifts. The effect of switching drifts off in the EDGE2D-EIRENE drift cases analyzed earlier in this paper is discussed in the present section.

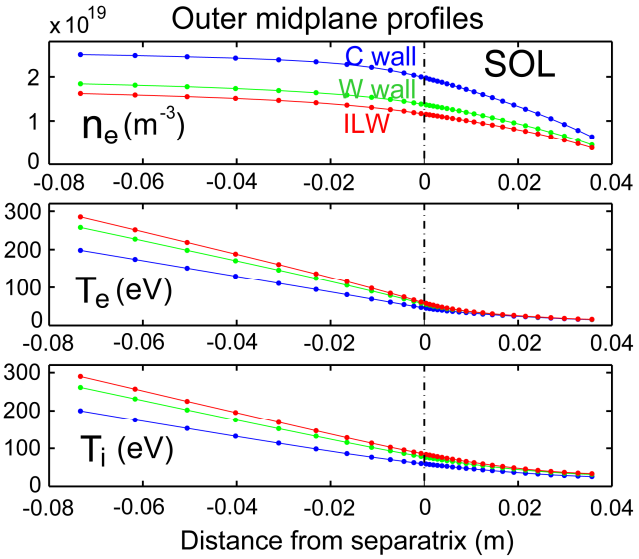

Fig. 6. Radial profiles of plasma parameters at the OMP position for non-drift cases.

OMP profiles of n_e, T_e and T_i for no-drift cases obtained by switching off drifts in the original drift cases (Fig. 2) are plotted in Fig. 6. Qualitatively they exhibit the same trends as in drift cases, except for a much more substantial difference between ILW and W wall cases. Such a change in the code output is influenced to a large degree by ionization of neutrals recycling in the divertor, with the latter in tum being influenced by asymmetries of plasma parameters between inner and outer divertors, see below. Divertor

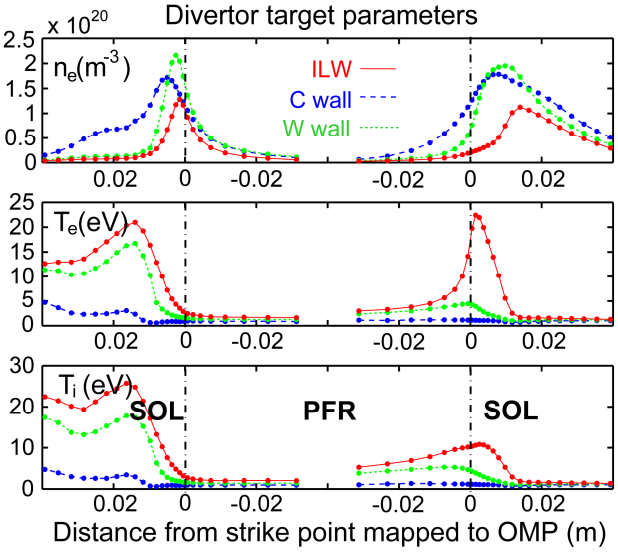

Fig. 7. Divertor target profiles vs. distance from strike points mapped to the OMP position for no-drift cases.

target profiles for no-drift cases are plotted in Fig. 7, for comparison with drifts cases shown in Fig. 3. Qualitatively, target profiles are similar to those in drift cases. Switching on drifts in the 'forward' toroidal field direction, with the ion ∇B drift directed towards the divertor, as in the cases presented in this paper, are known to increase T_e and T_i at the outer target while decreasing them at the inner target, with opposite shifts in electron density (see e.g. [26]). From Figs. 3 and 6 it follows that switching drifts on strongly reduces $T_{e,i}$ at the inner target between 0 and 0.01 m, leading to the n_e rise. Somewhat surprisingly, however, switching drifts on in the ILW case didn't lead to the $T_{e,i}$ rise, instead, the maximum outer target T_e went down from ≈ 20 to ≈ 15 eV, with the corresponding increase in n_e. This is most likely to be related to an increase in the recycling level in the drift ILW case, with the total neutral ionization rate of 2.86×10^{23} s^{-1} in the drift ILW case (see Sec. 4) substantially exceeding that in the no-drift case, 2.31×10^{23} s^{-1}. At the same time, for C and W cases, total ionization levels for drift and no-drift cases are almost the same, within 3%.

Neutral ionization source profiles for no-drift cases are plotted in Fig. 8, to be compared with Fig. 4 for drift cases. The W wall case profile is now clearly between ILW and C wall cases, in line with expectations based on the same trend in target profiles. The difference between the three no-drift cases is therefore quite clear, being seen in all figures presented here. At the same time, in drift cases the difference between ILW and W wall cases was partly masked by a substantial increase in the recycling level in the ILW case caused by switching on drifts, which in turn led to a higher neutral ionization source.

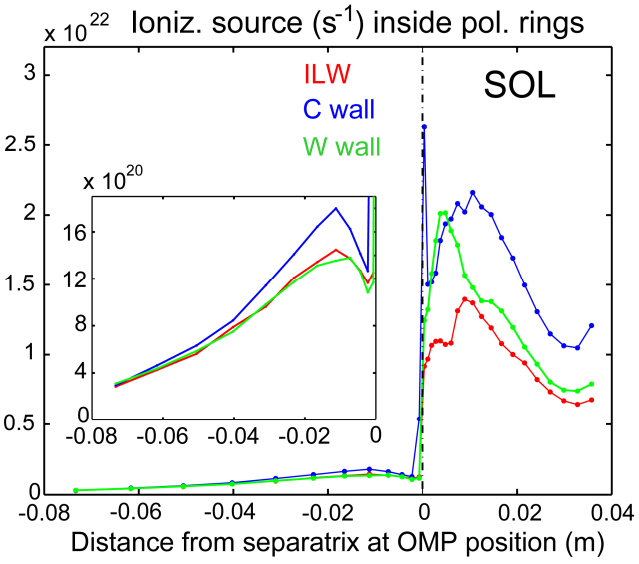

Fig. 8. The same neutral ionization source profiles as shown in Fig. 4, but for no-drift cases.

Ionization rates in the outermost cell of the SOL along OMP, indicative of ionization rate of neutrals reflected from the main chamber wall, are 0.84×10^{21}, 1.85×10^{21} and 1.32×10^{21} $m^{-3}s^{-1}$ for ILW, C and W wall cases, respectively. Qualitatively, they show a collinearity with the outermost points in Fig. 8 for the poloidally integrated ionization source. Since the latter is mainly determined by the ionization source in the divertor, such a collinearity indicated a link between neutral recycling levels in the divertor and in the main chamber wall.

Overall, differences in EDGE2D-EIRENE results among ILW, C and W wall cases are qualitatively the same for cases with and without drifts. This means that the physics behind these differences must not be related to drifts. The most significant differences are between metal wall (ILW and W wall) and C wall cases.

It has to be noted that there is one very important difference in the output between drift and no-drift cases in EDGE2D: electric fields are not calculated for no-drift cases, hence, the information on the radial electric field E_r is not available in them.

7. Lower density no-drift cases

The motivation for running EDGE2D-EIRENE cases at much lower densities, aimed at reducing large recycling in the divertor, was explained in Sec. 6. Owing to numerical instabilities, lower density cases with higher target T_e could only be run without drifts. No-drift EDGE2D-EIRENE cases however don't generate electric fields as a code output, so E_r profiles are not available in them, as pointed out above. One can therefore only check whether the trend for higher plasma density found in [13] will be repeated in EDGE2D-EIRENE cases.

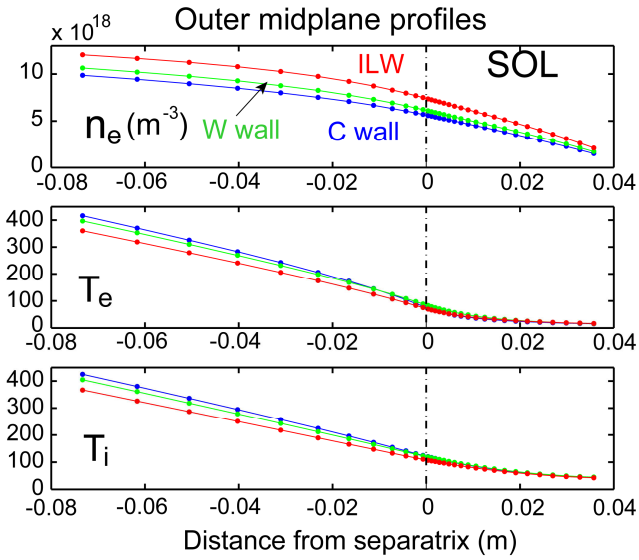

Fig. 9. Radial profiles of plasma parameters at the OMP position for lower density no-drift cases.

For running lower density EDGE2D-EIRENE cases the only change applied to the settings of no-drift cases analyzed in Sec. 6 was the reduction of the gas puff rate from 4.2×10^{21} to 1.0×10^{21} s^{-1}, leaving the same 'core fuelling rate' which is linked to the unchanged NBI heating power. This resulted in the inner core boundary density drop by factor ~ 2, as can be seen by comparing OMP profiles of lower density cases, plotted in Fig. 9 alongside T_e and T_i profiles, with those in normal density cases (the term 'normal' will be applied to cases with the 4.2×10^{21} s^{-1} gas puff, corresponding to JET experimental data and shown in Fig. 6. In a striking difference with Fig. 6, the C wall case density is lower than in metal wall cases. This is in line with expectations based on arguments used in [5] and modelling of low density cases in [13]. Such plasma parameters

however are not relevant for the L-H transition study because the plasma density is below that corresponding to a minimum in P_{LH} (see Fig. 1 of [8] showing density variation in the JET L-H transition study).

At the same time, against expectations based on the same arguments in [5,13], plasma density in the W wall case isn't the highest, being instead in between the other two cases and closer to the C wall case. This is despite W, specified also as the main chamber wall material in the W wall case, is much heavier than Be, specified as the main chamber wall material in the ILW case. This feature of the results will be discussed below.

Target profiles in lower density cases are plotted in Fig. 10. The factor ~ 2 reduction in OMP densities compared to normal density cases resulted in a factor ~ 10 reduction in peak target densities. Correspondingly, peak target T_e and T_i are much higher than in normal density cases, as total plasma pressure $n(T_e + T_i)$ tends to reach equilibrium along field lines. Target T_e profiles are peaked at strike points, with values being substantially higher than T_i owing to a much higher parallel electron heat conduction compared to that of ions.

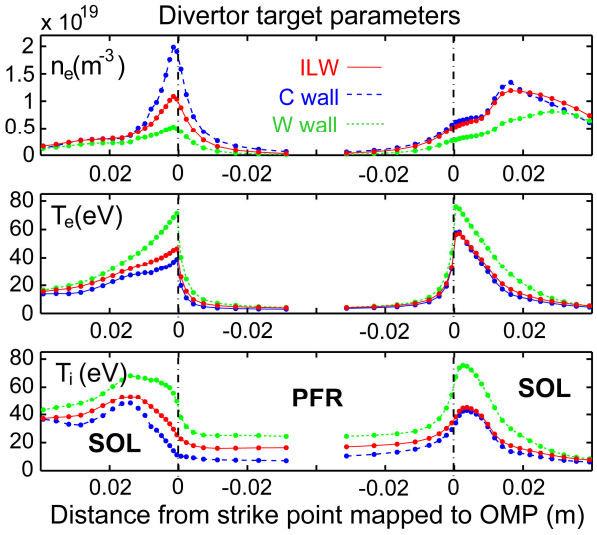

Fig. 10. Divertor target profiles vs. distance from strike points mapped to the OMP position, for lower density no-drift cases.

In difference with target profiles in normal density no-drift cases shown in Fig. 7, target densities in the W wall case are the lowest among the three cases, while target $T_{e,i}$ are the highest. The W wall case therefore has signatures of being the case with the lowers divertor recycling, which is not surprising since it has the highest atomic mass of the wall material all around the machine, leading to the lowest 'power deficit' and highest divertor temperatures. Surprisingly, however, highest energies of both ions and neutrals in the W wall case aren't translated into highest OMP densities. When comparing ILW and W wall cases, the only plausible explanation for such and unusual relation between their densities is that higher recycling in the divertor in the ILW case, caused by the presence of the low atomic mass Be as a material of the main chamber wall, makes a sizable contribution to the total neutral flux into the core and the ionization source there. This is possible because neutrals circulated near the main chamber wall and in the divertor are not fully decoupled from each other, being linked by

reflections from the walls and from the plasma via charge exchange processes.

Fig. 11 shows ionization source profiles for lower density no-drift cases. Compared to the profiles for the standard density no-drift profiles shown in Fig. 8, the fraction of the total ionization in the core is significantly higher, which is related to a large drop in the divertor recycling. The ionization source in the SOL is now the lowest in the W wall case. Despite this, the ionization source in the core in this case is higher than in the C wall case, in difference to situation in the standard density case (Fig. 8). The ionization pattern in the W wall case therefore demonstrates the largest re-balancing between the ionization in the SOL and in the core in favour of the latter, which can be easily explained by the lowest divertor recycling, highest $T_{e,i}$ in the divertor and highest neutral reflection coefficients from the main chamber wall (the latter – in comparison with the ILW case).

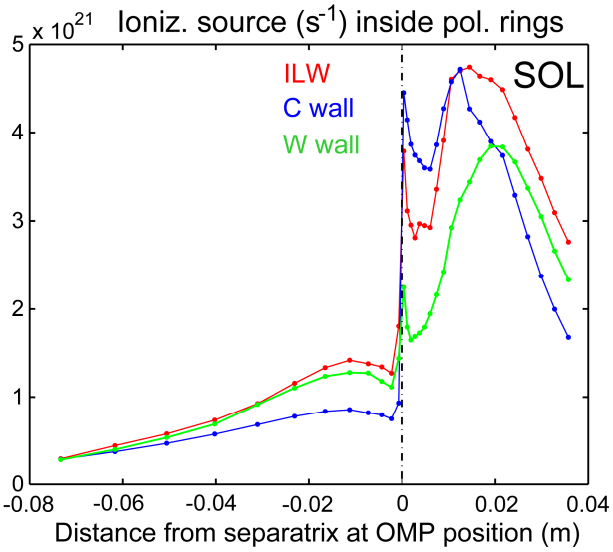

Fig. 11. The same neutral ionization source profiles as shown in Fig. 4, but for lower density no-drift cases.

Comparing ILW and W wall cases, one can see that the ionization source near the separatrix is higher in the ILW case, with the difference between the two cases being particularly large in the near SOL. This is the reason for a substantially higher separatrix density in the ILW case compared to the W wall case, see Fig. 9. This result is in a clear contradiction with the simple picture based on the assumption that higher atomic mass surfaces exposed to the interaction with the plasma and neutrals necessarily result in higher plasma densities in the core and at the separatrix. The presence of the lowest atomic mass material in the main chamber wall, Be, leads to higher divertor recycling and higher ionization in the vicinity of the separatrix, compared to the case with the W main chamber wall, resulting in higher separatrix density. This demonstrates the importance of the link between neutrals circulating in the main chamber wall and in the divertor as well as the impact of divertor recycling on core and separatrix density. Cooling of the SOL plasma triggered by the replacement of W with Be at the main chamber wall must have made its impact on the divertor plasma by reducing $T_{e,i}$, with the consequence of rising divertor recycling and leading to higher separatrix density. The cooling must be caused by both lower particle and energy reflection coefficients of ions and neutrals from Be surfaces. In particular, the

lower particle reflection coefficient implies that more impinging particles first get trapped in the surface and then being released from it as molecules at the very low, << 1 eV, surface temperature. This, compared to higher particle and energy reflection coefficients for the W surface, serves as power sink for the SOL plasma.

Similarly to the situation with normal density no-drift cases, ionization rates in the outermost cell of the SOL, along OMP, are equal to 2.25×10^{21}, 0.89×10^{21} and 1.56×10^{21} $m^{-3}s^{-1}$ for ILW, C and W wall cases, respectively. They are qualitatively collinear with integrated ionization sources in the in the outermost poloidal ring in Fig. 11. This again indicates a link between neutral recycling levels in the divertor and in the main chamber wall.

It has to be stressed that the interpretation of EDGE2D-EIRENE results, especially when comparing ILW and W wall cases, is challenging. It requires consideration of causality among several inter-connected physical mechanisms whose relative strength is not always easy to quantify. Among these mechanisms are:

- effect of deeper penetration of neutrals reflected from higher atomic mass materials into the plasma, raising core plasma density,
- impact of higher separatrix density on the $T_{e,i}$ reduction, density and neutral recycling increase in the divertor, resulting in higher neutral flux from the divertor into the core,
- effect of 'power deficit' in the divertor, related to lower energy reflection coefficients of neutrals from divertor surfaces with lower atomic mass and leading to lower divertor temperature(s), higher density and higher recycling,
- differentiation between effects of surface materials with different atomic masses in the divertor and in the main chamber wall, with neutrals reflected from the main chamber wall having more direct access to the core, in contrast with neutrals reflected from surfaces in the divertor; the latter, however, are capable of shifting the power balance in the divertor, thereby affecting the divertor recycling and neutral flux from the divertor into the core plasma,
- coupling between neutrals circulating near the main chamber wall and in the divertor via multiple reflections from walls and the plasma, as indicated by the link between neutral recycling levels in the divertor and in the main chamber wall.

An apparent conflict between the two different explanations given to opposite trends in OMP density profiles between ILW and W wall cases at normal and lower densities cannot be resolved in this paper. The explanations, especially the one given to higher OMP density in the ILW case in lower density cases, only provided arguments based on some, out of the whole list, of physics

mechanisms influencing the system. A detailed quantitative analysis, including analysis of energy spectra of neutrals at different locations around the torus and neutral pathways connecting different regions, will be required to resolve this issue. Such an analysis is beyond the scope of the present paper. It is possible that very different divertor conditions, with strong asymmetries between inner and outer divertors (note that the inner divertor in ILW and W wall normal density cases has low temperatures at the inner strike point, unlike in lower density cases) play an important role in the transport of neutrals. Finally, it is worth pointing out that the comparison between ILW and W cases at low densities could only be done for no-drift cases, while drifts can play an important role, especially in low density plasmas which have high target T_e and strongly peaked T_e profiles at strike points such as in the case of T_e profiles shown in Fig. 10 (see e.g. [26]).

EDGE2D-EIRENE cases were also run with a further reduction in the gas puff, from 1×10^{21} to 5×10^{20} s^{-1}. Separatrix densities in these cases were 5.6×10^{18}, 3.9×10^{18} and 4.2×10^{18} m^{-3} in ILW, C and W wall cases, respectively. Apart from lower densities and higher temperatures in the SOL, core and divertor regions, they didn't show any qualitative differences in OMP and target profiles, as well as in ionization patterns, among ILW, C and W wall cases, compared to the results presented in this section. This shows that all factors listed above pointing to complexity of the physics related to neutral recycling in the divertor and near the main chamber wall, with the key role played by (relatively high) divertor recycling in the neutral ionization rate in the core, can be applied to very low density plasmas.

8. Summary

EDGE2D-EIRENE modelling with drifts, based on the simulation of the JET L-mode discharge in ILW with the input NBI power close to the L-H transition, were carried out. Results of cases with exactly the same settings, but with two different wall materials: carbon (C) and tungsten (W), were compared with the original case in the ILW environment (with W covering surfaces in the divertor, and Be – in the main chamber wall). A significantly higher plasma density across core and SOL regions was obtained in the C wall case compared to metal wall cases (ILW and W). This is in a contradiction with experimental results from ASDEX Upgrade (AUG) [5,16], were plasmas in C and W wall environments were compared, as well as with results of the EMC3-EIRENE modelling [13], both pointing to higher density in W wall plasmas. AUG and EMC3-EIRENE results were interpreted via the effect of deeper penetration of neutrals reflected from surfaces with higher atomic mass material (W, due to higher particle and energy reflection coefficients compared to C) into the confined plasma. Deeper neutral penetration and ionization

was assumed to be responsible for higher core density and its gradient, ∇n, explaining experimental observations of lower H-mode power threshold in W wall plasmas. The latter was interpreted via an impact of ∇n on radial electric field E_r, with higher ∇n increasing E_r and its gradient resulting in turbulence suppression by the shear of the E×B rotation [5].

It has to be pointed out, however, that higher density and its gradient inside of the separatrix in the C wall case doesn't necessarily translate into higher E_r. On the contrary, in the EDGE2D-EIRENE modelling E_r is higher in metal wall cases, since it is more influenced by the gradient of ion temperature, ∇T_i, than by ∇n, provided input power and transport coefficients are the same in all cases. Hence, for unchanged pressure profiles in the core, as it is in the EDGE2D-EIRENE cases, higher ∇n in the C wall case results in lower E_r. Since divertor T_e is higher in metal wall cases, E_r in the near SOL, being formed to a large extent by Debye sheath potentials at the target, is also higher in metal wall cases. Thus, both 'inner' and 'outer' E_r (with respect to the separatrix position), are higher in metal wall cases, which correlates with lower H-mode threshold power in JET (with ILW) and AUG (with all W wall). It has to be noted that the dominance of the ∇T_i term over ∇n in the E_r formation is far from being granted in real experimental conditions. In particular, provided the extra neutral ionization forms the density profile with the ∇n increase by a much larger factor than for the density itself, the results on the comparison between E_r values in C and metal walls could be opposite to those described in this paper. Such conditions, however, should be considered rather exotic, or at least created only locally, applicable to some selected positions inside the separatrix, since ultimately it is the density gradient that causes an increase in the density itself, hence, these two quantities should evolve simultaneously and in the same direction.

Higher separatrix and core densities, as well as higher density gradient in the EDGE2D-EIRENE case in C is explained by the 'power deficit' in the divertor, with the lower energy reflection coefficient from C surfaces leading to more power flux absorbed by them, leaving less power available to heat the divertor plasma. A change in surface boundary conditions in the divertor is likely to trigger a positive feedback loop where lower $T_{e,i}$ in the divertor lead to higher divertor density and neutral recycling, further reducing $T_{e,i}$, and so on. The result is a substantially cooler and denser divertor plasma in the C wall case, with higher recycling and higher neutral flux into the core.

The mechanism of the core density rise by more energetic neutrals re-emitted from higher atomic mass surfaces, as discussed [5,13], shows itself up in EDGE2D-EIRENE cases with drastically reduced gas puff, from 4.2×10^{21} to 1.0×10^{21} s^{-1}, resulting in much lower plasma densities not

relevant to the L-H transition study. In these plasmas divertor recycling and the effect of the 'power deficit' in the divertor are apparently playing less important role, with the result that the EDGE2D-EIRENE cases with metal walls having higher separatrix and core densities than in the C wall case.

One of the most difficult EDGE2D-EIRENE results to interpret is the tendency for core and separatrix densities in W wall cases not continuing the trend established when transitioning from C wall to ILW cases, seen in both 'normal' density EDGE2D-EIRENE cases (based on the simulated JET L-mode case with the input power close to the H-mode power threshold) and in much lower density cases achieved by much lower gas puff rates. This was relatively easy to explain in 'normal' density cases, using arguments of Refs. [5,13] applied to neutrals reflected from the main chamber wall, predicting higher plasma density in the W wall compared to the ILW case. At the same time, at much lower densities it was the ILW case which had higher OMP density, and different mechanisms had to be invoked to provide a plausible explanation for the code results. Since these mechanisms are acting together, an explanation of such a different response of OMP density profiles to the W to Be main chamber wall changeover in high and low gas puff cases becomes challenging (see discussion near the end of Sec. 7). A detailed quantitative analysis, including analysis of energy spectra of neutrals at different locations around the torus and neutral pathways connecting different regions, as well as the analysis of the role of divertor in-out asymmetries and drift effects, is required to resolve this issue. Such an analysis is beyond the scope of the present paper.

Acknowledgement

Discussions with Drs. S.Brezinsek, D.P.Coster, E.Joffrin, C.Giroud, T.Lunt, C.F.Maggi, D.Moulton, P.A.Schneider, M.Wischmeier and E.Wolfrum are acknowledged. This work has been carried out within the framework of the EUROfusion Consortium and has received funding from the Euratom research and training programme 2014-2018 and 2019-2020 under grant agreement No. 633053. The views and opinions expressed herein do not necessarily reflect those of the European Commission.

References

[1] Martin Y R, Takizuka T and ITPA CDBM H-mode Threshold Database Working Group, 2008 J. Physics **123** 012033

[2] Righi E *et al* 1999 Nucl. Fusion **39** 309

[3] Maggi C F, Weisen H, Hillesheim J *C et al* 2018 Plasma Phys. Control. Fusion **60** 014045

[4] Maggi C F, Delabie E, Biewer T M *et al* 2014 Nucl. Fusion **54** 023007

[5] Shao L N , Wolfrum E, F Ryter F *et al* 2016 Plasma Phys. Control. Fusion **58** 025004

[6] Biglari H, Diamond P H and Terry P W 1990 Phys. Fluids B **2** 1

[7] Burrell K H 1977 Phys. Plasmas **4** 1499

[8] Delabie E *et al* 2015 42nd EPS Conf. on Plasma Physics (Lisbon, Portugal, 22–26 June 2015) paper O3.113 (http://ocs.ciemat.es/EPS2015PAP/pdf/O3.113.pdf)

[9] Chankin A V, Delabie E, Corrigan G *et al* 2017 Plasma Phys. Control. Fusion **59** 045012

[10] Simonini R *et al* 1994 Contrib. Plasma Phys. **34** 368

[11] Reiter D 1992 J. Nucl. Mater. **196-198** 80

[12] Wiesen S *et al* 2006 ITC Project Rep.

[13] Lunt T, Reimold F, Wolfrum E *et al* 2017 Plasma Phys. Control. Fusion **59** 055016

[14] Feng Y *et al* 2004 Contrib. Plasma Phys. **44** 57

[15] Feng Y *et al* 2014 Contrib. Plasma Phys. **54** 426

[16] Schneider P A, Barrera Orte L, Burckhart A et *al* 2015 Plasma Phys. Control. Fusion **57** 014029

[17] Roth J *et al* 2008 Plasma Phys. Control. Fusion **50** 103001

[18] Philipps V 2011 J. Nucl. Mater. **415** S2-S9

[19] Giroud C, Maddison G P, Jachmich S *et al* 2013 Nucl. Fusion **53** 113025

[20] Giroud C, 2020 private communication

[21] Coster D P, 2020 private communication

[22] Chankin A V, Coster D P, Corrigan G *et al* 2009 Plasma Phys. Control. Fusion **51** 065022

[23] Hazeltine R D 1974 Phys. Fluids **17** 961

[24] Cavedon M *et al* 2020 Nucl. Fusion **60** 066026

[25] Viezzer E *et al* 2014 Nucl. Fusion **54** 012003

[26] Chankin A V 1997 J. Nucl. Mater. **241-243** 199